

Circular particle fusion filter applied to map matching

ISSN 1751-956X
 Received on 3rd October 2016
 Revised 1st June 2017
 Accepted on 12th July 2017
 doi: 10.1049/iet-its.2016.0231
www.ietdl.org

Karim El Mokhtari¹ , Serge Reboul², Jean-Bernard Choquel², Georges Stienne², Benissa Amami¹, Mohammed Benjelloun²

¹Laboratoire d'Informatique, Système et Télécommunications, Université Abdelmalek Essaadi, Faculté des Sciences et Techniques, Ancienne Route de l'Aéroport, Km 10, Ziaten. BP: 416. Tangier, Morocco

²Laboratoire d'Informatique Signal et Image de la Côte d'Opale, Université du Littoral Côte d'Opale, EA 4491, 50, rue Ferdinand Buisson – F-62228 Calais, France

 E-mail: karim@elmokhtari.com

Abstract: Navigation in constrained areas such as ports or dense urban environments is often exposed to global navigation satellite system (GNSS) satellites masking caused by the infrastructures. In this case, the GNSS positioning is inaccurate or unavailable and proprioceptive sensors are generally used to temporarily localise the vehicle on a map. However, the drift of these sensors rapidly causes the navigation system to fail. In this study, the navigation is computed using magnetometer and GNSS observations defined in an absolute reference frame. The heading measurements are coupled with a digital map of the road network in order to localise the vehicle in a map matching process. The contribution of this study is the proposition of a particle filter that fuses the position and direction observations to estimate the vehicle position. In this context, when the GNSS signal is masked, the observations of direction are used to compute the vehicle position. The proposed filter is defined in both circular and linear domains in order to take into account the nature of the observations. The proposed approach is assessed on real and synthetic data.

1 Introduction

A map matching method fits the position provided by a global navigation satellite system (GNSS) receiver and a dead reckoning (DR) positioning system to a vector map. The aim of this approach is to find the corresponding road segment and to obtain the vehicle location. This technique is used for the navigation of cars and robots.

Several map matching approaches have been developed over the last years. They can be classified into different categories. The first considers the geometric relationships between the measured position and the map. We find in this category many approaches such as the ‘point-to-point’, ‘point-to-curve’, ‘curve-to-curve’ [1] and ‘area matching’ [2] algorithms. The second category considers, in addition to the geometry, the topology of the road network and the GNSS data history. Greenfeld proposes a weighted topological algorithm that is based on an analysis of the road network and GNSS data [3]; however, it does not consider any heading or speed information. Meng uses a topological analysis that relies on the correlation between the trajectory of the vehicle and the features of the road (turn, curvature, and connection) [4]. Meng's algorithm uses navigation data from GNSS/DR and spatial road network data including turn restrictions. This algorithm fails when the vehicle reaches junctions and switches to a post-processing mode which makes it unsuitable for real-time applications.

Other techniques have been applied to map matching, such as the probabilistic approach introduced by Honey *et al.* and extended by Zhao, Quddus [5], Kim *et al.* and Bierlaire *et al.* [6]. The goal of this approach is to model the sensors noise and take it into account in the map matching process. The fuzzy logic approach found in [7] considers the map matching as a process of decision based on rules representing expert knowledge on the road network. Nassreddine *et al.* [8] use belief theory in order to solve the multiple hypothesis problems that arise when the road segment has to be correctly chosen in the map matching problem. Toledo-Moreo *et al.* [9] propose a map matching process that uses an enhanced map to improve the vehicle localisation. In this approach the improvement is due to the use of a geometric roads description as a series of clothoids instead of linear segments. The global

approach presented by Brakatsoulas *et al.* considers the vehicle trajectory as a curve and the map matching as a problem of finding the road sequence that forms the closest curve to the trajectory using Fréchet distance [10]. This approach is only applicable offline when the whole trajectory is available. A comparative study of different classes of map matching algorithms can be found in [11].

The weight-based topological algorithm proposed by Quddus in [5, 12], denoted MAP-TOP, is used here as reference. It is an improvement of Greenfeld's algorithm. This map matching method was used by many authors ([13, 14]) and described in many studies such as [11] and more recently [15]. In this last study, the authors show that weight-based algorithms are more accurate than simple topological algorithms and less complex than advanced algorithms. They can be used for practical navigation applications since they are fast, easy to implement and do not need large memories. The MAP-TOP algorithm works with GNSS/DR and can be used in urban and suburban areas with a good accuracy [11]. It associates a weight to each road segment according to several criteria: the difference between the vehicle heading and the segments direction, the proximity of the vehicle position to the segments and the relative angular position of the segments. The segment with the highest score is chosen to map the current GPS fix. The matched position is the perpendicular projection of the GNSS fix on that segment.

Many of the map matching algorithms rely only on GNSS data and are unable to process the position when GNSS masking occurs. Moreover, the ambiguous cases of Y-junctions and parallel roads are not always clearly addressed. For example, the critical study in [15], which covers 22 map matching algorithms, shows that only 8 of them can handle GNSS masking by DR substitution. However, using DR as a positioning method quickly enlarges the uncertainty ellipse around the calculated position and therefore increases the space of probable roads.

In a recent study, authors in [16] propose a map matching algorithm that uses a fusion of GPS and DR data combined with a Switching Kalman Filter. Based on Hidden Markov Models, this filter aims at hypothesis tracking and validation. Although the approach is interesting for ambiguous situations such as parallel

roads and Y-junctions, the authors didn't take the case of an extended GPS masking into account. A fuzzy sorting map-matching algorithm is proposed in [17]. In this algorithm the grid index was used for candidate road sections filtering, and rectangle error regions were used instead of ellipses error. The proposed approach is only able to match GPS measurements, while the ambiguous situations as well as the masking case are not taken into account. Authors in [18] use KF to integrate GPS and 3D Reduced Inertial Sensor System in a loosely coupled fashion. Map matching is used to limit location errors during GPS outages. Their method uses geometrical Map matching (point-to-point matching and point-to-curve matching) to correct drifts due to the inertial sensors in the KF solution. These methods are influenced by outliers. In addition, the robustness of the algorithm with regard to the outage duration is not shown. In [1], a weighted topological algorithm is proposed to deal with poor GNSS signal quality without the use of inertial sensors. Even though the algorithm is able to correct map matching mismatches after a previous wrong decision, authors admit that the algorithm is greatly affected by the digital map precision and presents limitations in complex scenarios, mainly in Y-junctions and in case of frequent signal losses. Therefore GPS outage is only supported for short periods.

We can find in the published works several contributions about particle filtering for positioning in urban environment. Most of these works focus on sensor hybridisation and fusion in Non Line Of Sight (NLOS) and multi-path situations where GNSS observations are unavailable or corrupted. The fusion and nonlinear filter aim at combining DR information with GNSS observations in order to guaranty the continuity of the position estimation. The DR sensors non-linearities are associated with the drift and biases that are estimated and removed in a particle filter [19, 20]. Many works also consider multipath rejection and mitigation with nonlinear filtering. The aims of such filters are to detect multipath and to estimate the associated bias in the GNSS pseudorange in order to correct the estimated position [21, 22]. Several map matching implementations with a particle filter were proposed in the literature. In [9, 23], the aim of the particle filter is to use the nonlinear model associated to an accurate representation of the map with splines and clothoids. In [24], raw GPS measurements are used to match the vehicle position in the map. In this work, the particle filter aims at solving the multi-hypothesis problem associated to the propagation of the particles in the road network. In [25, 26], a continuous and accurate system based on deadreckoning sensors, a map and a GNSS receiver is proposed. In this case, the particle filter allows considering sensors providing data based on non-linear models and to incorporate the map in the estimation process. In all of these works the observations of positions are provided by a GNSS receiver. In this work we propose to also use the heading observations associated to the map to locate the vehicle. In our filter, the propagation of the particles is constrained on the road network. When the vehicle heading is changing, in accordance with a change of a road segment direction, the particles are reconcentrated at the beginning of the new segment and the position is obtained.

In this paper, we propose a map matching approach that uses heading observations to localise a vehicle on a digital map. The proposed map matching process is implemented in a particle filter. The heading measurements, defined in a global reference frame, are independent of the GNSS signals availability. When the GNSS receiver cannot provide observations of positions, the observed heading measurements are used to estimate the position. In this case, the heading measurements are matched to the road directions defined by the digital map in order to process the position. In this implementation, the digital map describes the road topology with segments. When the GNSS observations are available, the proposed approach fuses the observations of position with the observations of direction to process the vehicle location. The proposed filter ensures the continuity of the process of map matching in the absence of GNSS signals.

The organisation of the paper is as follows: after the presentation of the map matching process in Section 2, we describe in Section 3 the particle map matching implementation used to

estimate the vehicle position. The assessment on synthetic and real data is presented in Section 4. A conclusion ends the article.

2 Map matching process

For our map matching implementation we assume that we have GNSS observations of the positions with observations of speed and direction. We choose to only use sensors that provide observations defined in a global reference frame. A GNSS receiver provides the position observations (in the WGS 84 Geodetic System) and a magnetometer provides the heading observations (a measurement of orientation with respect to the magnetic North). These orientation observations are associated to a map to locate the vehicle in the turns (in the WGS 84 Geodetic System).

The state model describes the evolution of the vehicle position $(x(t), y(t))^T$, the vehicle direction $\theta(t)$ and the variation of vehicle direction $\Delta\theta(t)$. For the map matching case, we propose an additional state variable $r(t)$ which defines the current road identity. $r(t)$ is the road segment number. The direction $\alpha(r(t))$ is defined with coordinates of the road segments included in the map database. Therefore, we describe the state model by the following equations:

$$\begin{aligned} x(t) = & x(t-1) + v(t)\Delta t \cos(\alpha(r(t-1))) \\ & + \eta_x(t) \cos(\alpha(r(t-1))) \end{aligned} \quad (1)$$

$$\begin{aligned} y(t) = & y(t-1) + v(t)\Delta t \sin(\alpha(r(t-1))) \\ & + \eta_y(t) \sin(\alpha(r(t-1))) \end{aligned} \quad (2)$$

$$\theta(t) = \theta(t-1) + \Delta\theta(t-1) + \eta_\theta(t) \quad (3)$$

$$\Delta\theta(t) = \Delta\theta(t-1) + \eta_{\Delta\theta}(t) \quad (4)$$

$$r(t) = r(t-1) + \eta_r(t) \quad (5)$$

where $\eta_r(t)$ is a noise with a discrete uniform distribution on the road numbers connected to the current segment, $\eta_x(t)$ and $\eta_y(t)$ are Gaussian centred noises, $\eta_\theta(t)$ and $\eta_{\Delta\theta}(t)$ are noises with a circular normal distribution. In this system, the velocity $v(t)$ is a command.

In the proposed model the novelty is to use a circular distribution for the state-transition-model and for the measurement model of the direction. This distribution allows taking into account the circularity of the data and more particularly to suppress the discontinuities associated to the transitions between $-\pi$ and π . In this case it is possible to consider the vehicle direction as a state variable.

The measurements of direction provided by a magnetometer act as observations for the state filter. The following equation models the measurements provided by the magnetometer:

$$\phi(t) = \theta(t) + \eta_\phi(t) \quad (6)$$

where $\eta_\phi(t)$ is an additive circular normal random variable [27] that models the noise on the heading observations.

The positions provided by the GNSS receiver also act as observations. The following equations model the measurements of position:

$$xp(t) = x(t) + \eta_{xp}(t) \quad (7)$$

$$yp(t) = y(t) + \eta_{yp}(t) \quad (8)$$

where $\eta_{xp}(t), \eta_{yp}(t)$ are additive normal random variables that model the noise on the observations of positions. This classical noise model for the observed position does not take the effect of possible multipath occurrences into account: multipath estimation and/or rejection is out of the scope of this paper.

A recursive state filter based on the state equations and the measurement equations would compute the two following steps:

- i. Prediction: We predict the position on the road network, the direction and the segment identity with the state equations.
- ii. Update:

- (a) Update the direction. The estimated direction is the one that minimises the filter innovation between the observation $\phi(t)$ and the predicted direction.
- (b) Update the segment identity with the identity of all the segments connected to the current segment. In this case, the estimated value of $r(t)$ is the one that minimises the filter innovation between the estimated direction and $\alpha(r(t))$.
- (c) Update the position. The estimated position is the one that minimises the filter innovation between the predicted position and the GNSS observation.

Unfortunately the strong non-linearity of the state and measurement models does not allow an implementation with an extended Kalman filter. We propose to implement the estimator of the state *a posteriori* law knowing the measurement in the form of a Gaussian-circular particle filter. The choice of the particle filter is motivated by the system non-linearity. The Gaussian statistic model is associated to the observations of positions. The description in the circular domain is motivated by the direction observations evolving between $-\pi$ and π . The von Mises distribution (or circular normal distribution) is the circular equivalent of the normal distribution in the linear domain [27]. This distribution is 2π -periodic. Its probability density function $f_{CN}(\theta; \mu, \kappa)$ for a circular variable θ , with mean μ and concentration parameter κ is given by:

$$f_{CN}(\theta; \mu, \kappa) = \frac{1}{2\pi I_0(\kappa)} e^{\kappa \cos(\theta - \mu)} \quad (9)$$

where I_0 is the modified Bessel function of the first kind and order zero.

3 Particle map matching implementation

3.1 Introduction

In this section the proposed map matching implementation is presented. The algorithm relies on a particle filter implementation. The position $(\hat{x}_t, \hat{y}_t)^T$ on the road network, the identity of the current segment \hat{r}_t and the direction of the vehicle $\hat{\theta}_t$ are estimated. This estimation is realised with the observations of direction ϕ_t provided by a magnetometer and the positions $(z_{x,t}, z_{y,t})^T$ provided by a GNSS receiver.

A particle filter represents the possible candidates for the parameters to estimate with a set of particles. A position on the vector map, a direction and a road segment identity is associated to each particle. In the prediction step, the particles are propagated with the state transition model. In the update step, a weight is computed for each particle. In our implementation there are two sets of weights; a set of weights for the direction and another one for the position. The first set of weights is used to estimate the direction and the second set is used to estimate the position and the segment identity. The novelty of the proposed approach is to use the direction for the processing of the position. The proposed technique for the segment identity propagation allows moving the particle from one segment to another segment. In this case, the particle segment identity is used to process the weights for the position estimation because it concentrates the particles on the segments that have the direction closest to the estimated direction. When the vehicle is turning, the particles are reconcentrated at the beginning of the new road segment and provide at this instant an absolute positioning (independent of the drift of the state model). In the proposed implementation when the GNSS position is available these two position information are fused.

3.2 Map matching algorithm

i. Initialisation:

To initialise the particles, N positions are drawn according to a bi-dimensional normal distribution centred on $(z_{x,0}, z_{y,0})$, the first observation of position. The positions are orthogonally projected on the closest segments to derive the particles of positions $(X_0^i, Y_0^i)^T$ and the particles which define the initial segment identity R_0^i .

ii. Prediction step:

The particles are propagated on the roads network segments using the following equations:

- Propagation of the position:

$$\begin{aligned} X_t^i &= X_{t-1}^i + v_{t-1} \Delta t \cos(\alpha(R_{t-1}^i)) \\ &\quad + \nu_{v,t}^i \cos(\alpha(R_{t-1}^i)) \end{aligned} \quad (10)$$

$$\begin{aligned} Y_t^i &= Y_{t-1}^i + v_{t-1} \Delta t \sin(\alpha(R_{t-1}^i)) \\ &\quad + \nu_{v,t}^i \sin(\alpha(R_{t-1}^i)) \end{aligned} \quad (11)$$

where $\nu_{v,t}^i$ is a random noise that models the uncertainty on v_{t-1} . $\nu_{v,t}^i$ follows a uniform distribution of mean zero and variance $\nu_{v,Q}$. R_{t-1}^i defines the road segment associated to the particle i at instant $t-1$.

- Propagation of the road identity:

$$R_t^i = f(R_{t-1}^i, X_t^i, Y_t^i) \quad (12)$$

If a particle leaves the current segment, a new identity and position is defined.

The function $f(\dots)$ is defined in three steps. In a first step, it is decided whether the particle is still on the current segment. The classical approach that uses the vector and scalar product of the particle position $(X_t^i, Y_t^i)^T$ with the current segment provides this information. In a second step, if the particle has left the current segment, its new identity is drawn according to a discrete uniform distribution among the identities of all the roads connected to the end of the current segment. In a third step the position of the particle (X_t^i, Y_t^i) is projected on this new segment.

- Propagation of the direction:

We define a set of particles Θ_k^i and $\Delta\Theta_k^i$ in order to respectively estimate the direction and the variation of direction.

$$\Theta_k^i = \Theta_{k-1}^i + \Delta\Theta_{k-1}^i \quad (13)$$

$$\Delta\Theta_k^i = \Delta\Theta_{k-1}^i + \nu_{\theta,t}^i \quad (14)$$

where $\nu_{\theta,t}^i$ is a random noise that follows a circular normal distribution of mean zero and variance $\nu_{\theta,Q}$.

iii. Direction estimation :

- Update step: The weights used to estimate the current direction are calculated with the observations of direction provided by the magnetometer.

$$\tilde{w}_{\theta,t}^i = w_{\theta,t-1}^i f_{CN}(\phi_t; \Theta_k^i, \kappa_{R_\theta}) \quad (15)$$

where κ_{R_θ} is the concentration parameter of the von Mises distribution f_{CN} . To give a probabilistic meaning to the weights, they are normalised as follows:

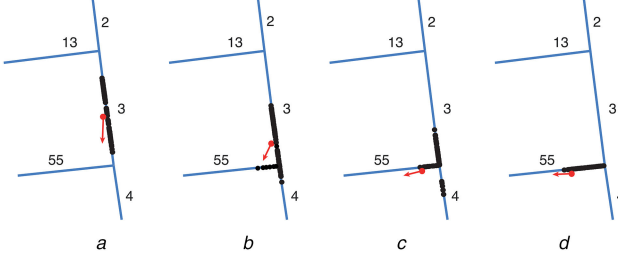


Fig. 1 Behaviour of the particle filter in a turn

$$w_{\theta,t}^i = \frac{\tilde{w}_{\theta,t}^i}{\sum_{i=1}^N w_{\theta,t}^i} \quad (16)$$

- Estimation: The vehicle direction $\hat{\theta}_t$ is computed with the particles weight by the following formula:

$$\hat{\theta}_t = \arg \left(\sum_{i=1}^N w_{\theta,t}^i \exp(j\Theta_t^i) \right) \quad (17)$$

iv. Position estimation :

- Update step: The weights used to estimate the current position are calculated with the estimated heading direction and the observations of position provided by the GNSS receiver.

$$\begin{aligned} \tilde{w}_{p,t}^i &= w_{p,t-1}^i f_N \left(\left| (z_{x,t}, z_{y,t})^T - (X_t^i, Y_t^i)^T \right| \right), \\ &\quad R_N f_{CN}(\hat{\theta}_t; \alpha(R_t^i), \kappa_R) \end{aligned} \quad (18)$$

where κ_R , the concentration parameter of the von Mises distribution $f_{CN}(\dots)$, indicates our tolerance to a road segment with a direction different from the estimated heading direction. R_N is the variance of the Gaussian distribution $f_N(\dots)$. The weights defined with the product $f_N(\dots) f_{CN}(\dots)$, realise the fusion of the measurements provided by the magnetometer and the GNSS receiver. When the GNSS observations are unavailable, the weights are only defined with the estimated direction as follows:

$$\tilde{w}_{p,t}^i = w_{p,t-1}^i f_{CN}(\hat{\theta}_t; \alpha(R_t^i), \kappa_R) \quad (19)$$

The weights are normalised as follows:

$$w_{p,t}^i = \frac{\tilde{w}_{p,t}^i}{\sum_{i=1}^N \tilde{w}_{p,t}^i} \quad (20)$$

- Estimation: The vehicle road segment identity is derived from the estimated position obtained with the weights as follows:

$$\hat{r}_t = g \left(\sum_{i=1}^N w_{p,t}^i X_t^i, \sum_{i=1}^N w_{p,t}^i Y_t^i \right) \quad (21)$$

where \hat{r}_t is defined with the function $g(x, y)$ as the segment the nearest to the position $(x, y)^T$.

Finally the vehicle position is derived with the following function :

$$(\hat{x}_t, \hat{y}_t)^T = l \left(\sum_{i=1}^N w_{p,t}^i X_t^i, \sum_{i=1}^N w_{p,t}^i Y_t^i, \hat{r}_t \right) \quad (22)$$

where $l(x, y, \hat{r}_t)$ is the projection of the position $(x, y)^T$ on the estimated road segment with identity \hat{r}_t .

v. Resampling :

In our implementation we use the Sequential Importance Resampling (SIR) [28] with an effective number of particles defined as follows:

$$N_{eff\theta} = \frac{1}{\sum_{i=1}^N w_{\theta,t}^i} \quad (23)$$

$$N_{effp} = \frac{1}{\sum_{i=1}^N w_{p,t}^i} \quad (24)$$

In this process, the particles with a high weight are duplicated and the number of particles with a low weight is decreased.

3.3 Case of the absence of GNSS data

When the GNSS receiver cannot provide observations to the map matching algorithm, the heading observations are used to estimate the position. In this case the estimated position is computed with the weights used for the estimation of the segment identity. These weights are defined with the likelihood value of the heading observation $\hat{\theta}_t$ compared to the predicted particle segment direction α . These weights give more importance to the particles on segments with the same direction as the vehicle displacement.

We note here that the key parts of this algorithm are when the vehicle performs a rotation manoeuvre. This manoeuvre helps the algorithm to concentrate the particles around the point where a change of segment occurs. When all the particles are located on the same segment, their weights are the same and the filter predicts the particles positions without corrections.

The example illustrated in Fig. 1 shows the behaviour of the particle filter in the absence of GNSS data and when the vehicle enters a turn. The actual position of the vehicle and its direction are respectively represented by a red circle and a red arrow.

4 Methods evaluation

4.1 Introduction

In this section, we assess the proposed method for 4 different scenarios. In each scenario, we compare our method (denoted MAP-SIR) with the topological map matching algorithm proposed in [5, 12] (denoted MAP-TOP).

- In the first scenario, we consider a Y-shape intersection shown in Fig. 2 and a simulated trajectory along the roads of this intersection. Through 1000 realisations of this trajectory, we assess our method in terms of position accuracy and correct road identification.
- In the second scenario (Fig. 4), we use a digital map in vector format of the city of Calais in France provided by the OpenStreetMap website [29]. We assume that the vehicle travels over a path generated with real data on the roads referenced in this map. In this scenario, we assess our method in terms of correct road identification for different GPS error values and for different GPS masking durations.
- In the third scenario (Fig. 5), we use a path generated by real data to assess the two algorithms in a trajectory with frequent turns.
- In the fourth (Fig. 7), we use real data obtained in the field to assess the position accuracy and correct road identification for different GPS masking durations.

We report in Table 1 the parameters settings for the different scenarios. For the MAP-TOP algorithm, $\Delta\beta'$ and α are, respectively, the thresholds used to detect the vehicle rotation and the segment's end (refer to [12] for more details).

In the simulations, the error on the measured direction is distributed according to a centred von Mises distribution. The concentration parameter is fixed to $\kappa = 30$ in order to model the inaccuracy of a low-cost magnetometer. The error on the velocity is assumed to be Gaussian and biased. The variance is set to 1 m/s and the bias is assumed to follow a uniform distribution between

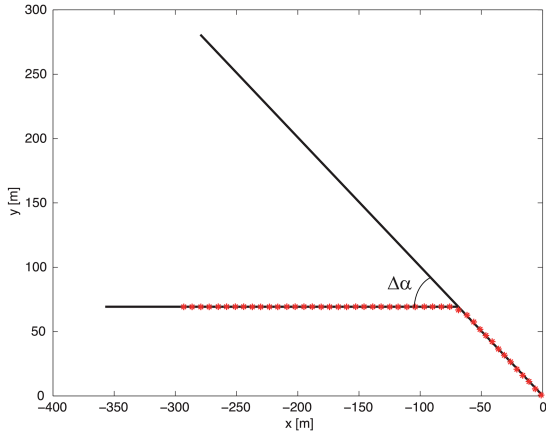


Fig. 2 Y-shape intersection

Table 1 Filters parameters for all scenarios

$\Delta\alpha, {}^\circ$	45	34	22	11
particle filter on direction				
N	200	200	200	200
$\kappa_{R\theta}$	10	10	10	10
MAP-SIR				
N	200	200	200	200
κ_R	100	100	100	100
R_N	σ_{GPS}	σ_{GPS}	σ_{GPS}	σ_{GPS}
ν_Q	9	9	9	9
MAP-TOP				
threshold $\Delta\beta'$, degree	45	34	22	11
threshold α , degree	90	90	90	90

0.5 and -0.5 m/s. The GPS positioning inaccuracy is modelled with an additive random value on the coordinate components distributed according to a Gaussian distribution of mean zero. The standard deviation of this bi-dimensional density, σ_{GPS} , is the same for the two components. The GPS error in this case, is the mean distance between the observations and the true position. This error is supposed to encompass all the errors relative to the position processing by the GPS receiver.

4.2 Scenario 1: Y-shape intersection

We consider the Y-shape intersection illustrated in Fig. 2. We simulate a trajectory starting at the lower-right corner (point of coordinates $(0, 0)$). The vehicle travels with a constant velocity of 10 km/h (~ 3 m/s). The intersection is reached at time $t = 50$ s. The vehicle turns right and continues moving on the horizontal road to the left. In this experimentation we consider noisy observations of the direction and of the velocity.

4.2.1 Position estimation: To assess the positioning accuracy, we define the position error as the average of the distance between the real position and the estimated position.

When the GPS is masked along the whole trajectory, we show the position error over time in Fig. 3a for each algorithm. We also calculate the position error for each realisation (average of the positioning error for all the trajectories per realisation), depicted in Fig. 3b. The results obtained in Figs. 3a and b show that the positioning is improved by the proposed MAP-SIR filter because the error is smaller per realisation and over time after the bifurcation. However, we can observe on Fig. 3a that the position error of the MAP-SIR filter becomes higher than the MAP-TOP algorithm when the vehicle approaches the bifurcation ($t = 50$ s). This is explained by the fact that the particles are still propagated on the previous segment because the junction is detected with a delay due to the pre-filtering of the observed directions. We also note that the proposed algorithm allows reducing the position error

to 3.5 m after the bifurcation. This reduction corresponds to the position correction with the direction. The error of 3.5 m is associated with a detection delay of approximately two seconds with a vehicle traveling at 2.7 m/s and a sampling rate of one second.

To assess the robustness of the proposed method, we process the global position error which is the average of the distance between the real and the estimated positions calculated over the whole trajectory and for 1000 realisations of the Y-shape trajectory. This error is processed for different values of the bifurcation angle $\Delta\alpha$.

We report in Table 2 this error in meters for each value of $\Delta\alpha$ when the GPS is masked along the whole trajectory.

The results reported in Table 2 show that the proposed filter is more accurate than the traditional approach. The positioning error obtained with the proposed algorithm is indeed always lower than the error obtained with the conventional method for all the assessed bifurcation angles $\Delta\alpha$.

We report in Table 3 the global position error as a function of the standard deviation of the GPS error when the GPS signals are available for the whole trajectory.

The results reported in Table 3 show that the fusion of the observations of directions and positions with the proposed filter is more accurate than the traditional approach all the assessed GPS errors.

4.2.2 Road identification: We estimate the probability of correctly identifying the segment on which the vehicle is located.

When the GPS is masked along the whole trajectory, we show in Fig. 3c this probability according to the position of the vehicle on the trajectory. We note that the proposed algorithm allows detecting a change of road identity at the junction much faster than the classical algorithm MAP-TOP. The probability to correctly identify the road is indeed higher when the vehicle is close to the junction.

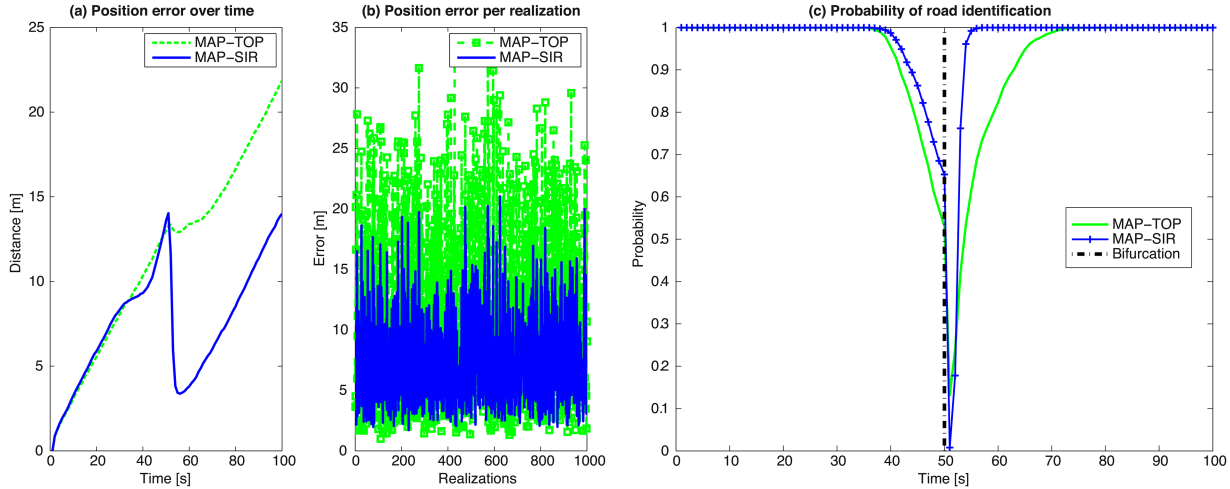


Fig. 3 Position error and road identification probability when the GPS is masked along the whole trajectory. The bifurcation angle is $\Delta\alpha = 45^\circ$

Table 2 Global position error and probability of identification for different bifurcation angles when the GPS is masked along the whole trajectory

$\Delta\alpha$, degree	45	34	22	11
global position error in meters				
MAP-TOP, m	11.2	12.0	14.4	14.8
MAP-SIR, m	8.1	8.0	8.7	9.5
probability of identification				
MAP-TOP	0.915	0.895	0.801	0.772
MAP-SIR	0.943	0.946	0.937	0.926

Table 3 Global position error and probability of identification for different GPS errors and $\Delta\alpha = 45^\circ$

GPS error in, m	1.2	2.5	6.4	12.4	18.7	24.8
global position error in meters						
MAP-TOP, m	0.81	1.63	4	7.96	11.95	15.91
MAP-SIR, m	0.69	1.1	1.91	3	3.87	4.7
probability of identification						
MAP-TOP	0.98	0.97	0.96	0.93	0.91	0.89
MAP-SIR	0.99	0.99	0.98	0.97	0.97	0.97

To assess the overall performance of the identification we calculate the probability to identify the correct segment on the entire trajectory. We report in Table 2 this probability for each value of $\Delta\alpha$ when the GPS is masked along the whole trajectory. We report in Table 3 this probability as a function of the standard deviation of the GPS error for $\Delta\alpha = 45^\circ$.

The results described in Tables 2 and 3 show that the proposed method is more robust than the MAP-TOP approach because it provides a higher road identification probability whether the GPS observations are available or masked.

4.3 Scenario 2: evaluation in a real context

We consider an experimentation in a real context defined in Fig. 4. In this case, the vehicle path is generated with real data. The distance travelled by the vehicle is 580 m, for a duration of 125 s (125 GPS fixes at 1 Hz). As illustrated in Fig. 4, GPS signal masking can occur at a random starting point and last for a chosen duration.

In a first experiment, the GPS signals are always available. We consider different GPS errors to assess the positioning accuracy. We report in Table 4 the global position error obtained by both methods. This error is estimated with 100 realisations of the trajectory and for different GPS errors.

We observe that the positioning error obtained with the proposed algorithm is always lower than the error obtained with the conventional method for all the assessed GPS errors. The results presented in Table 4 confirm the interest of the proposed fusion filter.

In a second experiment, we compare the two algorithms when the masking is partial. We mask n consecutive GPS observations at a random starting point on the trajectory. For each value of n , we generate 1000 realisations of the experiment. We report in Table 5 the estimated percentage of correctly identified segments for each percentage of masked points.

In this experimentation we show the influence of the filter initialisation. In both cases, the last available point before a masked area is given by the GPS position. For both methods, in the masked area, the proprioceptive sensors measurements are used to localise the vehicle. The error of initialisation at the beginning of a masked area plus the drift of the proprioceptive sensors degrade the MAP-TOP algorithm accuracy. With the MAP-SIR approach, the particles are disseminated on all the segments that surround the last available point. In this context, the MAP-SIR filter that uses the vehicle direction as observation concentrates its particles along the correct segment. Furthermore, at each turn the particles are concentrated on the true location of the road corner and correct in this case the drift of the sensors. The results presented in Table 5 show that the proposed method is more robust in the masked area thanks to the heading map matching and the better filter initialisation.

4.4 Scenario 3: trajectory with frequent turns

In this scenario, we consider the trajectory shown in Fig. 5 characterised by frequent turns. Position, velocity and heading are given by real data. GPS masking occurs during the whole trajectory. Both GPS and DR trajectories are shown in Fig. 5. We

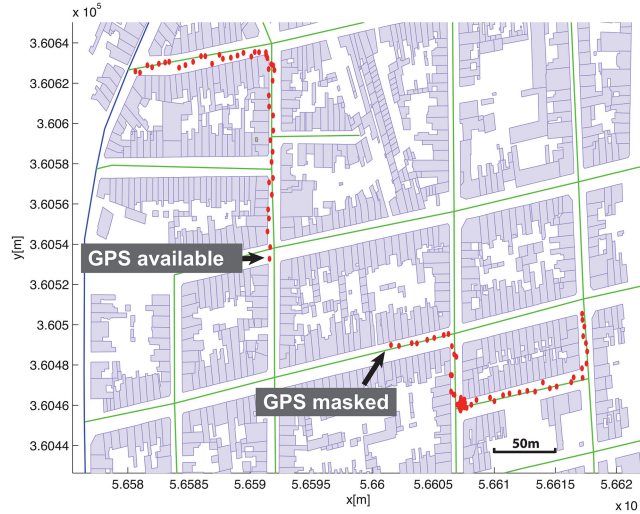


Fig. 4 Trajectory of the vehicle showing an example of GPS masking

Table 4 Global position error as a function of the percentage of masked points

Masked points in %	6	23	41	58	76	90
The standard deviation of the GPS error is 12.4 m						
MAP-TOP, m	8.6	8.6	9.0	9.2	9.1	9.7
MAP-SIR, m	2.3	2.4	2.6	2.7	2.9	3.1
The standard deviation of the GPS error is 1.2 m						
MAP-TOP, m	0.8	1.1	1.6	2.3	3.0	4.0
MAP-SIR, m	0.7	1.1	1.5	1.8	2.3	2.7

Table 5 Percentage of correctly identified segments as a function of the percentage of masked points

Masked points in %	6	23	41	58	76	90
The standard deviation of the GPS error is 12.4 m						
MAP-TOP in %	0.87	0.87	0.85	0.85	0.84	0.83
MAP-SIR in %	0.98	0.98	0.98	0.98	0.98	0.98
The standard deviation of the GPS error is 1.2 m						
MAP-TOP in %	0.99	0.98	0.97	0.96	0.94	0.93
MAP-SIR in %	0.99	0.98	0.97	0.96	0.96	0.96

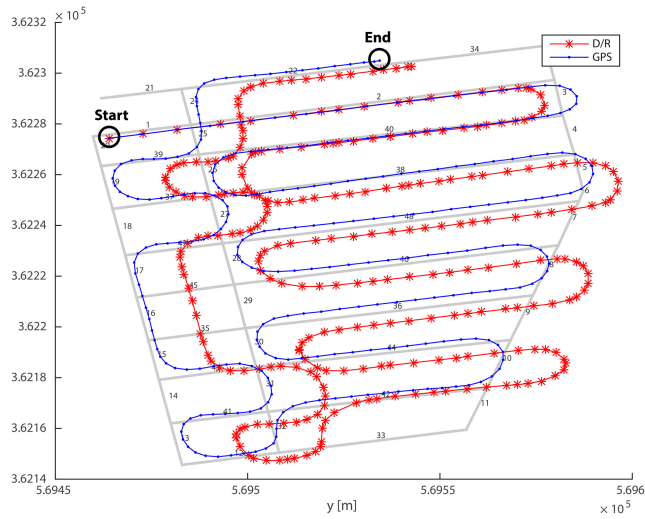


Fig. 5 Trajectory with frequent turns

execute 100 Monte Carlo runs of the noise on velocity and heading.

We show in Fig. 6a the error on position for the studied algorithms. We observe that the error increases over time for the MAP-TOP algorithm, whereas it remains globally below 10 m for MAP-SIR. The repetitive falls on the error curve of MAP-SIR are due to turn detection as explained above. With regard to road

identification, Fig. 6b shows that MAP-SIR performs better than MAP-TOP especially after a long period of masking. The MAP-SIR algorithm stays almost close to a probability of 1 except during turns where it reacts more rapidly than MAP-TOP as observed previously in the Y-junction experiment.

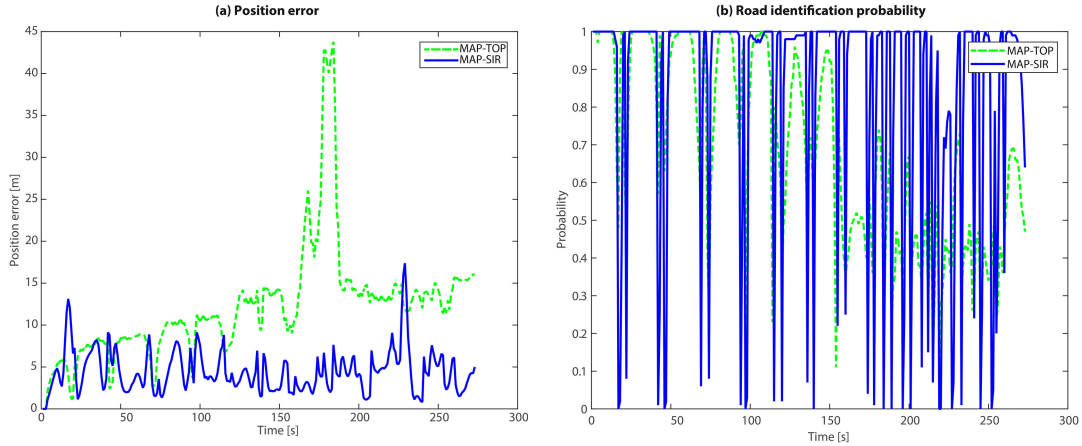


Fig. 6 Position error and road identification probability

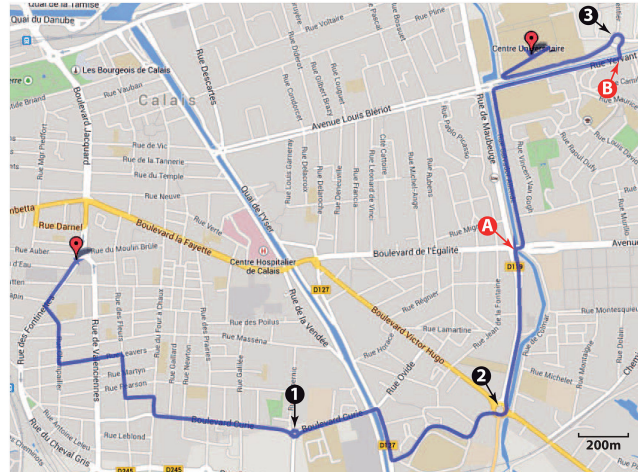


Fig. 7 Vehicle trajectory in the experiment with real data

Table 6 Percentage of correctly identified segments as a function of the percentage of masked points

Masked points in %	6	23	41	58	76	90
MAP-TOP in %	98.0	83.8	68.2	50.7	38.5	17.8
MAP-SIR in %	98.4	92.4	85.0	73.6	67.4	55.5

4.5 Scenario 4: application to real data

4.5.1 Experimental context: The experimentation with real data was performed using an instrumented vehicle equipped with a magnetometer to measure the vehicle direction, an optical velocity sensor and a GPS receiver. To decrease the ferromagnetic perturbations of the vehicle, the magnetometer is placed at the centre of gravity of the car and at equal distance between the roof and the floor. A calibration of the direction provided by the magnetometer is realised at the beginning of the trajectory.

The trajectory shown in Fig. 7 was conducted in the city of Calais in France. It has a duration of 14 min 20 s and the travelled distance is 5.6 km. The vehicle crosses three roundabouts numbered (1)–(3) in Fig. 7. It makes a complete rotation on the roundabout (1). It stops twice at the red lights denoted (A) and (B) during respective time periods of 68 and 34 s.

The frequency of the GPS receiver is 0.5 Hz, the velocity and direction measurements are obtained with a frequency of 2 Hz. The path contains 1720 direction and velocity measurements and 430 GPS points.

4.5.2 Methods evaluation: We assess the performance of the MAP-SIR filter and the MAP-TOP algorithm. The parameters settings are:

- MAP-TOP algorithm: We keep the parameter values given in Table 1.

- MAP-SIR filter: $\kappa_Q = 1 \times 10^3$, $\kappa_{\bar{Q}} = 1 \times 10^4$, $\kappa_R = 800$. This last parameter was increased compared with the experiment in Section 4.3 because the noise on the measured angle is lower. We consider a concentration parameter $\kappa_{R_p} = 1$ for the von Mises distribution used to assign weights to the particles. This parameter is smaller than the one used in previous experiments (see Table 1) to enable the filter to explore more roads.

We want to evaluate the performance of each approach as a function of n , the number of masked GPS measurements. In this context, we randomly generates 100 starting points for each n consecutive masked points. We then evaluate for each algorithm the percentage of correctly identified segments in Table 6 and the average of the distance between the GPS position and the estimated position in Table 7. The results presented in Tables 6 and 7 show that the propose approach is more accurate and robust than the classical approach.

4.5.3 Discussion of an ambiguous case: An interesting advantage of the MAP-SIR filter compared with the classical topological algorithm is observed in the ambiguous case of the two parallel roads 3 and 4 shown in Fig. 8. This turn can be found between roundabouts (1) and (2) in Fig. 7 where roads 3 and 4 are on both sides of a river. In this case, the vehicle crosses the bridge (road 2) in step (a) then turns to road 4. The turn in the trajectory calculated by DR is located on the river between the two parallel

Table 7 Average distance between the GPS position and the estimated position as a function of the percentage of masked point

Masked points in %	6	23	41	58	76	90
MAP-TOP, m	1.0	16.2	43.0	86.0	136.6	191.9
MAP-SIR, m	2.2	6.7	12.6	17.6	19.7	23.7

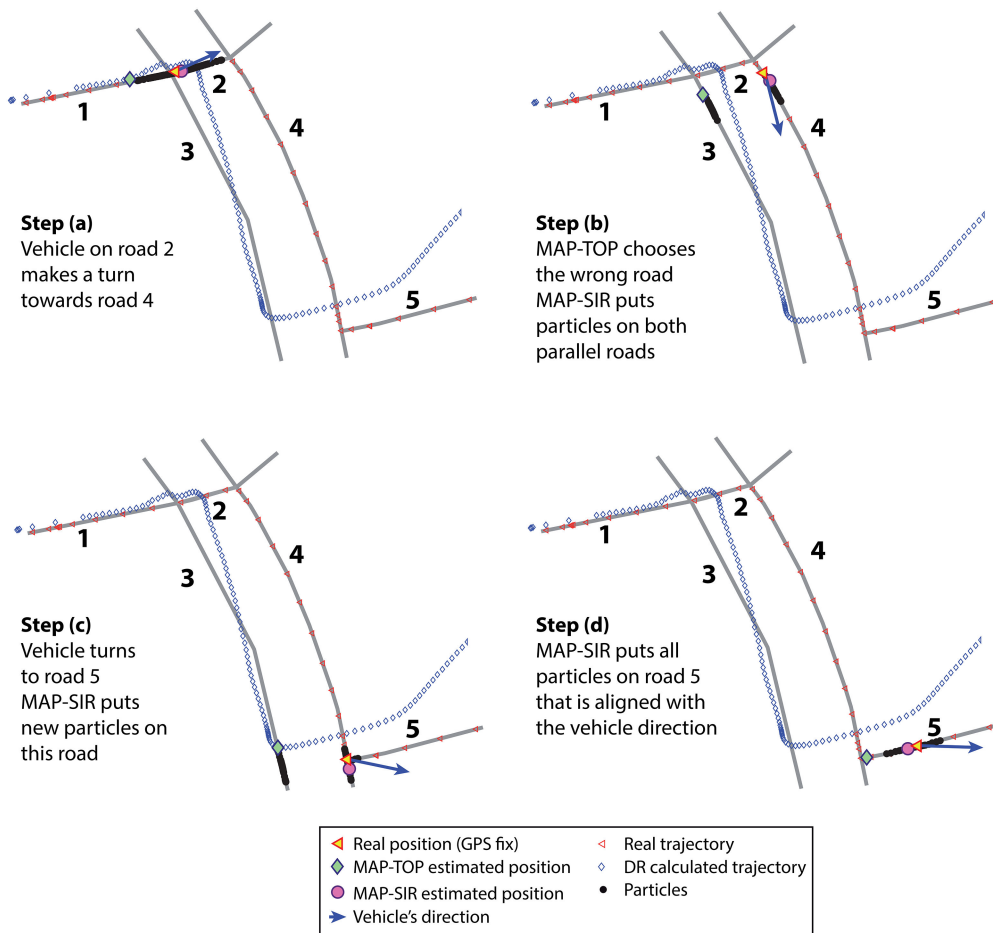


Fig. 8 Ambiguous case of parallel roads

roads 3 and 4 which brings an ambiguity to the decision making. After the turn is completed in step (b), the MAP-TOP algorithm chooses the wrong road 3 because it is closer to the position given by DR. The MAP-SIR filter, however, places particles on the two roads 3 and 4 as they have almost equal probability given the movement direction. The estimated position depends on the road on which a higher number of particles exists [road 4 in our case]. The two groups of particles continue to evolve independently on the parallel roads until the vehicle turns to road 5 (step (c)). Since it is not possible to make such a turn on road 3, particles on this road are assigned a lower weight, then replaced by new ones on road 5. In this way, the particle filter can handle ambiguities found mainly in parallel roads and Y-junctions and correct anterior wrong matching.

5 Conclusion

In this paper, we propose a map matching approach that uses heading and position observations to localise a vehicle on a digital map. The proposed map matching technique is implemented in a particle filter that processes both linear and circular data.

The proposed filter estimates simultaneously the vehicle direction, the vehicle position and the identity of the road where the vehicle is currently positioned. It can process the vehicle positions with the observations of direction, used as observation of position, even when the GNSS signal is not available. Furthermore, it takes into account the digital map in the positioning process by

propagating the particles of positions on all the roads segments connected to the current road.

In the experimentation, we show that the particle map matching filter provides better results than the conventional topological map matching algorithm. On synthetic data, we show that the error on the estimated position is lower and that the road identification at a bifurcation is faster. In addition, we show that the proposed method is more robust to noise with any bifurcation angle values. In the experimentation with real data we show that the proposed filter is more accurate in terms of positioning and reliable in terms of road identification for different masking periods.

6 References

- [1] Jimenez, F., Monzon, S., Naranjo, J.E.: ‘Definition of an enhanced map-matching algorithm for urban environments with poor GNSS signal quality’, *Sensors*, 2016, **16**, p. 193
- [2] Lianxia, X., Quan, L., Minghua, L., *et al.*: ‘Map matching algorithm and its application’. Proc. of the Int. Conf. on Intelligent Systems and Knowledge Engineering (ISKE), 2007
- [3] Wang, W., Jin, J., Ran, B., *et al.*: ‘Integrated map matching algorithm for GPS-based freeway network traffic monitoring’. Transportation Research Board 89th Annual Meeting, 2010
- [4] Quddus, M., Washington, S.: ‘Shortest path and vehicle trajectory aided map-matching for low frequency GPS data’, *Transp. Res. C*, 2015, **55**, pp. 328–339
- [5] Quddus, M.A.: ‘High integrity map matching algorithms for advanced transport telematics applications’. Ph.D. dissertation, Imperial College, London, UK, 2006
- [6] Bierlaire, M., Chen, J., Newman, J.: ‘A probabilistic map matching method for smartphone GPS data’, *Transp. Res. C*, 2013, **26**, pp. 78–98

- [7] Ren, M., Karimi, H.A.: ‘A fuzzy logic map matching for wheelchair navigation’, *GPS Solut.*, 2012, **16**, (3), pp. 273–282, doi: 10.1007/s10291-011-0229-5
- [8] Nassreddine, G., Abdallah, F., Denoeux, T.: ‘Map matching algorithm using belief function theory’. Proc. of the 11th Int. Conf. on Information Fusion (FUSION ‘08), 2008, pp. 995–1002
- [9] Toledo-Moreo, R., Betaille, D., Peyret, F., *et al.*: ‘Fusing GNSS, dead-reckoning, and enhanced maps for road vehicle lane-level navigation’, *IEEE J. Sel. Top. Signal Process.*, 2009, **3**, (5), pp. 798–809
- [10] Parent, C., Spaccapietra, S., Renso, C., *et al.*: ‘Semantic trajectories modeling and analysis’, *ACM Comput. Surv.*, 2012, **45**, (4), pp. 42:1–42:32
- [11] Quddus, M.A., Ochieng, W.Y., Noland, R.B.: ‘Current map-matching algorithms for transport applications: state-of-the art and future research directions’, *Transp. Res. C: Emerg. Technol.*, 2007, **15**, (5), pp. 312–328
- [12] Quddus, M.A., Ochieng, W.Y., Zhao, L., *et al.*: ‘A general map matching algorithm for transport telematics applications’, *GPS Solut.*, 2003, **7**, (3), pp. 157–167
- [13] Velaga, N.R., Quddus, M.A., Bristow, A.L.: ‘Developing an enhanced weight-based topological map-matching algorithm for intelligent transport systems’, *Transp. Res. C: Emerg. Technol.*, 2009, **17**, (6), pp. 672–683
- [14] Haiqiang, Y., Shaowu, C., Huifu, J., *et al.*: ‘An enhanced weight-based topological map matching algorithm for intricate urban road network’, *Procedia – Soc. Behav. Sci.*, 2013, **96**, pp. 1670–1678
- [15] Hashemi, M., Karimi, H.A.: ‘A critical review of real-time map-matching algorithms: Current issues and future directions’, *Comput. Environ. Urban Syst.*, 2014, **48**, pp. 153–165
- [16] Smaili, C., El Badaoui El Najjar, M., Charpillet, F.: ‘A hybrid Bayesian framework for map matching: Formulation using switching Kalman filter’, *J. Intell. Robot Syst.*, 2014, **74**, pp. 725–743
- [17] Wu, Q., Gu, X., Luo, J., *et al.*: ‘A vehicle map-matching algorithm based on measure fuzzy sorting’, *J. Comput.*, 2014, **9**, pp. 1058–1065
- [18] Cossaboom, M., Georgy, J., Karamat, T., *et al.*: ‘Augmented Kalman filter and map matching for 3D RIIS/GPS integration for land vehicles’, *Int. J. Navig. Observ.*, 2012, **2012**, pp. 1–16
- [19] Gustafsson, F., Gunnarsson, F., Bergman, N., *et al.*: ‘Particle filters for positioning, navigation and tracking’, *IEEE Trans. Signal Process.*, 2002, **50**, (2), pp. 425–437
- [20] Caron, F., Davy, M., Duflos, E., *et al.*: ‘Particle filtering for multisensor data fusion with switching observation models: application to land vehicle positioning’, *IEEE Trans. Signal Process.*, 2007, **55**, (6), pp. 2703–2719
- [21] Giremus, A., Tourneret, J.Y., Calmettes, V.: ‘A particle filtering approach for joint detection/estimation of multipath effects on GPS measurements’, *IEEE Trans. Signal Process.*, 2007, **55**, (4), pp. 1275–1285
- [22] Rabaoui, A., Viandier, N., Duflos, E., *et al.*: ‘Dirichlet process mixtures for density estimation in dynamic nonlinear modeling: application to GPS positioning in urban canyons’, *IEEE Trans. Signal Process.*, 2012, **60**, (4), pp. 1638–1655
- [23] Kuhnt, F., Kohlhaas, R., Jordan, R., *et al.*: ‘Particle filter map matching and trajectory prediction using a spline based intersection model’. 17th Int. IEEE Conf. on Intelligent Transportation Systems (ITSC), Qingdao, 2014, pp. 1892–1893
- [24] Fouque, C., Bonnifait, P.: ‘Matching raw GPS measurements on a navigable map without computing a global position’, *IEEE Trans. Intell. Transp. Syst.*, 2012, **13**, (2), pp. 887–898
- [25] Davidson, P., Collin, J., Takala, J.: ‘Application of particle filters to a map-matching algorithm’, *Gyroscopy Navig.*, 2011, **2**, (4), p. 285
- [26] Georgy, J., Noureldin, A., Goodall, C.: ‘Vehicle navigator using a mixture particle filter for inertial sensors/odometer/map data/GPS integration’, *IEEE Trans. Consum. Electron.*, 2012, **58**, (2), pp. 544–552
- [27] Jammalamadaka, S.R., SenGupta, A.: ‘Topics in circular statistics’ (World Scientific Publ., New Jersey, 2001)
- [28] Arulampalam, S., Maskell, S., Gordon, N., *et al.*: ‘A tutorial on particle filters for online nonlinear/Non-Gaussian Bayesian tracking’, *IEEE Trans. Signal Process.*, 2002, **50**, pp. 174–188
- [29] OpenStreetMap website. Available at <http://www.openstreetmap.org>